



Universiteit  
Leiden  
The Netherlands

## Vortex Motion Study of Oxidised Superconducting NbRe Microstrips

Chen, X.; Cirillo, C.; Eijrnaes, M.; Parlato, L.; Pepe, G.P.; Attanasio, C.; ... ; Dood, M.J.A. de

### Citation

Chen, X., Cirillo, C., Eijrnaes, M., Parlato, L., Pepe, G. P., Attanasio, C., ... Dood, M. J. A. de. (2023). Vortex Motion Study of Oxidised Superconducting NbRe Microstrips. *Ieee Transactions On Applied Superconductivity*, 34(3). doi:10.1109/TASC.2023.3340641

Version: Publisher's Version

License: [Licensed under Article 25fa Copyright Act/Law \(Amendment Taverne\)](#)

Downloaded from: <https://hdl.handle.net/1887/3716629>

**Note:** To cite this publication please use the final published version (if applicable).

# Vortex Motion Study of Oxidised Superconducting NbRe Microstrips

Xingchen Chen, Carla Cirillo, Mikkel Ejrnaes, Loredana Parlato, Giovanni Piero Pepe, Carmine Attanasio, Sense Jan van der Molen and Michiel J. A. de Dood

**Abstract**—We report measurements of the flux flow instability velocity in 8nm thin superconducting NbRe microstrips. In particular, a change in vortex motion after the film has been lightly oxidised is observed. We propose a possible mechanism according to which pinning is caused by domain walls where the superconducting properties are discontinuous and support our claim by a toy-model time-dependent Ginzburg-Landau simulation. Since our model is very general and applies to any type-II superconductor, we expect similar effects on other air-sensitive polycrystalline thin film superconductors.

**Index Terms**—Vortex flow, vortex pinning, superconducting critical current, thin film superconductor, superconducting microstrip, superconductivity in magnetic field

## I. INTRODUCTION

**I**N type-II superconductors the magnetic field can penetrate into the superconducting state in the form of the flux quanta. This is commonly known as vortex entry [1]. Due to the Lorentz force, the vortices can move freely within the superconductor. The study of the dynamic vortex regime provides a platform to comprehend nonequilibrium-correlated physics [2] [3]. Furthermore, it is of great importance for the application of superconducting devices that operate at near-critical currents [4]–[6].

Under vortex-free conditions, before the superconductor reaches the depairing current, the superconducting state can be destroyed locally due to the local impurity or certain geometry [7]. In the presence of vortices, however, the dynamic vortices cause low energy dissipation well inside the superconducting state. Experimentally this is commonly measured as a resistive state before the Cooper-pair-depairing current is reached. Typically, the energy dissipation is solely induced by the viscous vortex flow, the measured resistive states have highly nonlinear current-voltage (I-V) correlations [8]. A discontinuous jump to the normal state is observed at a current known as the flux-flow instability point. At this point, the vortices are moving at

the maximum velocity that can be sustained in the presence of the damping force [9].

Assuming uniformly distributed quasiparticles across the sample, Larkin and Ovchinnikov predicted theoretically that the instability flow velocity  $v$  is independent of the magnetic field as long as the diffusion length of the quasiparticle is larger than the triangular vortex lattice constant  $a(B)$ . At smaller fields, this translates to  $v\tau \propto a(B) \propto B^{(-1/2)}$ ,  $\tau$  is the quasiparticle relaxation time [3] [10]. In the presence of pinning centers provided either by specific device geometry or structural defects, however, the commonly used relation no longer holds [10]–[13].

In the presence of local defects and variations, the quasiparticle diffusion is no longer homogeneous across the sample, instead, the diffusion is only uniform along the direction of the specific flow direction [10]. This results in a distribution of the vortex flow velocity where the velocity depends heavily on the location of the specific vortex. Through measuring the dissipation, only the average flow velocity can be obtained.

With increasing magnetic field the flux flow instability velocity increases, as more and more vortices start to interact with one another, weakening the pinning effect. The flux-flow instability velocity reaches a maximum at a certain magnetic field. Beyond this field more vortices are pushed into the sample, making the quasiparticle distribution more and more uniform, and the flux-flow velocity stabilises, recovering to the  $B^{-1/2}$  dependency.

NbRe thin films have been recently proposed as a promising superconducting material for the realization of single photon detectors [14] [15]. This was indeed confirmed in NbRe-based devices made both in the forms of nanowires [16] and microstripe [17] [18]. For a high-quality 15 nm thin film, the instability flow velocity was reported to exceed 500 m/s at high fields, corresponding to a quasiparticle relaxation time of about 100 ps [14], putting them well within the range of popular Superconducting Nanowire Single Photon Detector (SNSPD) materials such as NbN [19], NbTiN [20] [21], MoSi [22] and WSi [23].

Here, we report a reduction in flux flow velocity that we interpret as pinning behaviour in lightly oxidised 8 nm NbRe film. The surface defects, act as pinning centres, and change the flux-flow behaviour of the film. In fact, for a clean polycrystalline film, the flux flow instability velocity is measured to saturate around 450 m/s at high fields, whereas in the oxidised film, a strong pinning effect for vortex flow with a maximum saturation flow velocity of about 200 m/s near  $T_c$  is observed.

We emphasise the importance of long-term prevention of

Manuscript received September 19, 2023; revised December 19, 2023. (Corresponding author: Xingchen Chen and Michiel J. A. de Dood)

Xingchen Chen (email: chen@physics.leidenuniv.nl), Sense Jan van der Molen and Michiel de Dood (email: dood@physics.leidenuniv.nl) are with Huygens-Kamerlingh Onnes Laboratory, Leiden University, P.O. Box 9504, 2300 RA Leiden, The Netherlands

Carla Cirillo is with CNR-SPIN, c/o Università di Salerno- Via Giovanni Paolo II, 132 - 84084 - Fisciano (SA), Italy

Mikkel Ejrnaes is with CNR-SPIN, Via Campi Flegrei, 34, 80078 Pozzuoli NA, Italy

Loredana Parlato and Giovanni Piero Pepe are with Dipartimento di Fisica “E. Pancini,” Università degli Studi di Napoli Federico II, I-80125 Napoli, Italy

Carmine Attanasio is with Dipartimento di Fisica “E. R. Caianiello,” Università degli Studi di Salerno, I-84084 Fisciano, Salerno, Italy

oxidation in fabricating a NbRe-based nanowire single photon detector. The decrease in flux flow instability velocity corresponds directly to an increase in the quasiparticle relaxation time. This limits the minimum required recovery time of an SNSPD as well as the timing jitter. For applications, a well-designed cover layer that prevents slight oxidation will be required.

## II. METHOD

8 nm thin NbRe films were sputtered with a DC diode magnetron sputtering system onto a  $SiO_x(300nm)/Si$  substrate in  $10 \times 10^{-3}$  mbar Ar background. The sputtering target is 99.9% pure bulk  $Nb_{0.20}Re_{0.80}$  [24]. Devices were created using negative resist and electron beam lithography and patterned using an Ar plasma in an ion beam etcher.

The device geometry is shown in figure 1, where the outer two probes are used as current leads while the inner two probes are used to measure voltage. All microstrips have a length of  $10 \mu m$ , but the width of the microstrip varies from  $1.8 \mu m$  to  $4.8 \mu m$ . During measurements, all magnetic fields are out of the plane, normal to the device surface.

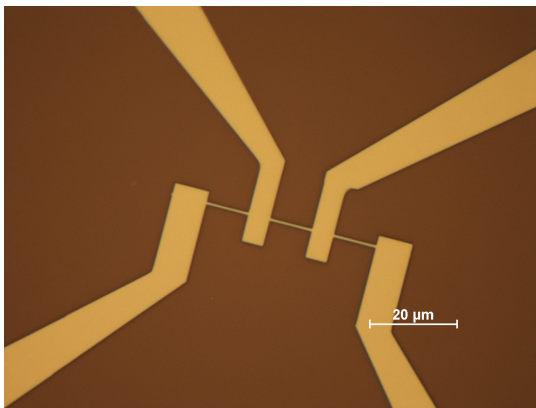


Fig. 1. Optical microscope image of a typical device ready to be measured. The strip width shown in the figure is  $1.8 \mu m$ .

## III. RESULTS

We first present results for an unoxidized film. Figure 2 shows measured IV curves as a function of magnetic field strength on a log-log scale for a device of width  $3.3 \mu m$  measured at 3.0 K. The flux flow dissipates energy before the abrupt jump to normal state resistance of the devices. The jump corresponds to the flux flow instability and the last points before the jump are used to calculate vortex instability velocity  $v = V/(BL)$  where  $V$  is the measured voltage,  $B$  is the magnetic field and  $L$  is the device length.

At the higher magnetic field, the uncertainty in finding the instability point becomes increasingly larger due to the mixing of contributions from both the localised normal transition and vortex flow to the energy dissipation. The blue dashed line in figure 2 highlights the field at which the step-like transition in energy dissipation becomes increasingly gradual. This is also reflected in the calculated results of instability velocity in magnetic fields.

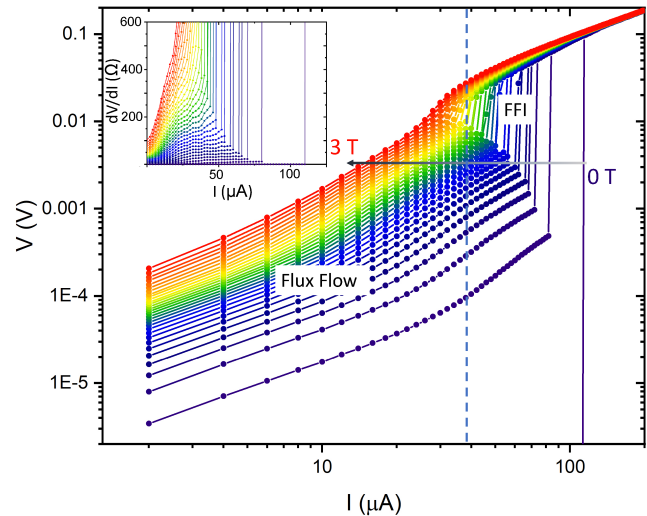


Fig. 2. IV curves of a  $3.3 \mu m$  wide NbRe microstrip measured at  $T=3.0$  K. The different curves correspond to a magnetic field that increases from  $B=0$  T to 3 T in steps of 0.1 T. The flux flow and flux flow instability region are marked in the graph before the linear region of normal device resistance. The blue dashed line indicates where the sudden jump to normal state resistance becomes gradual-like. Insert is the differential resistance obtained for each measured IV curve.

The vortex instability velocity found from the data in Figure 2 is plotted in figure 3. The red line is based on the Bardeen-Stephen model and serves to guide the eye. The velocity reaches values of about 500 m/s at smaller fields and stabilises around 450 m/s at larger fields ( $B > 1.5$  T). Our results are well-matched with previously measured data on a slightly thicker film [16]. The fast vortex instability velocity corresponds to a very short quasiparticle relaxation time, supporting the claim that thin film NbRe is a promising candidate for fast and efficient single-photon detection with SNSPDs [25]–[27].

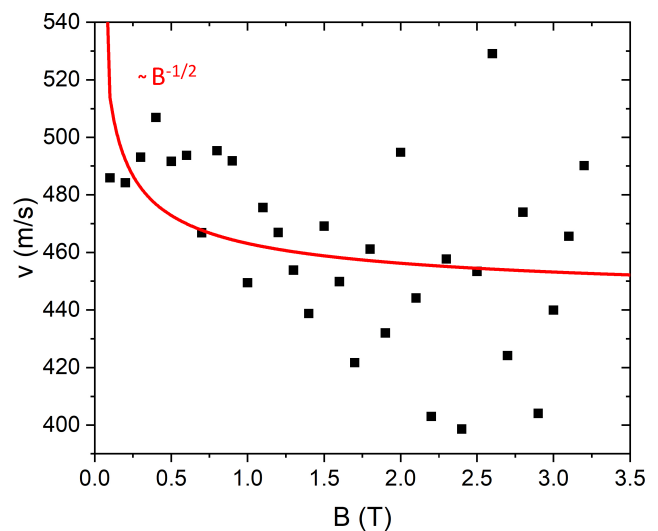


Fig. 3. Instability velocity derived from figure 2 as a function of out-of-plane magnetic field. The black dots show the experimental data and the red curve represents the Bardeen-Stephen model and serves to guide the eye.

When the etched devices are left in contact with the air

for 3 hours, the oxidation will slowly vary the film surface condition from polycrystalline to amorphous oxides. Although the superconductivity still survives, the flux motion becomes nonuniform and this impacts the diffusion of quasiparticles.

The detailed measurements of the magnetic response of a  $1.8 \mu\text{m}$  wide device at 2.5 K are shown in figure 4 as a typical result for lightly oxidised devices. At each individual field, the vortices go through pinning, normal flow, instability and eventually a jump in the IV-curve to normal state resistance with increasing current. The different regimes for vortex motion are marked in the figure.

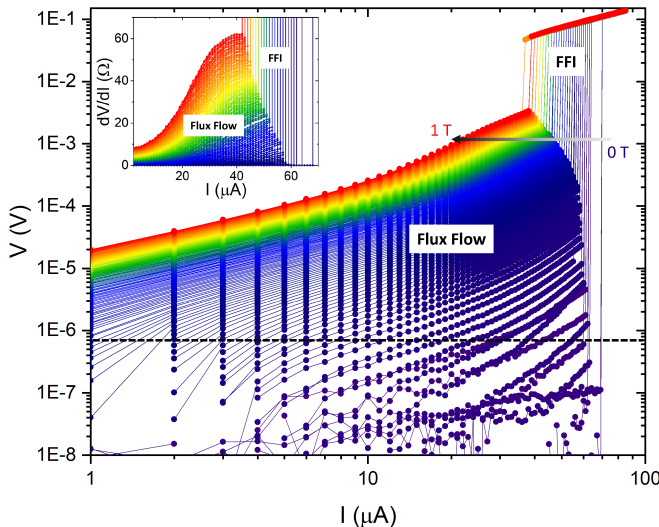


Fig. 4. IV curves of an oxidised  $1.8 \mu\text{m}$  wide device with increasing magnetic field in steps of 0.01 T measured at 2.5 K. The different regions of flux motions are marked in the graph. Insert is the differential resistance calculated with the measured IV curve, the same regions are indicated.

From the data, it is clear that the measured voltage for the flux flow region on the lightly oxidised film is much lower than that of the unoxidised film, indicating a much smaller energy dissipation. We interpret these results as the presence of extra pinning centres for vortices across the devices. The difference in vortex motion can also be seen in the differential resistance graph (insert in Figure 4), where a flattening in the differential resistance is present before the jump to the normal state.

The flux flow instability velocity as a function of the magnetic field behaves in a completely different manner compared to the previous results. Figure 5 shows the vortex instability velocity as a function of the magnetic field for several different devices at different temperatures. The colours of the markers represent the temperature while the shape of the markers indicates different devices. The square and round symbols correspond to  $4.8 \mu\text{m}$  and  $2.2 \mu\text{m}$  wide microstrips, respectively.

The data in Figure 5 do not follow the  $B^{-1/2}$  trend observed in Figure 3 at any temperature. Instead, at lower magnetic fields the instability velocities are small and only start to increase at magnetic fields around 20 mT and saturate at about 180 m/s for fields of 1.0 T. This is even more pronounced in the data for a microstrip device that is  $1.8 \mu\text{m}$  wide shown

in the insert of Figure 5, where at low temperature (2.0 K) the velocity stays well below 5 m/s for fields below 70 mT. The flux flow instability velocity of the unoxidised film shown in Figure 3 is similar to what had been observed in superconductors that present heavy pinning behaviour where the unrestricted movement of vortices is disrupted by pinning centers [28].

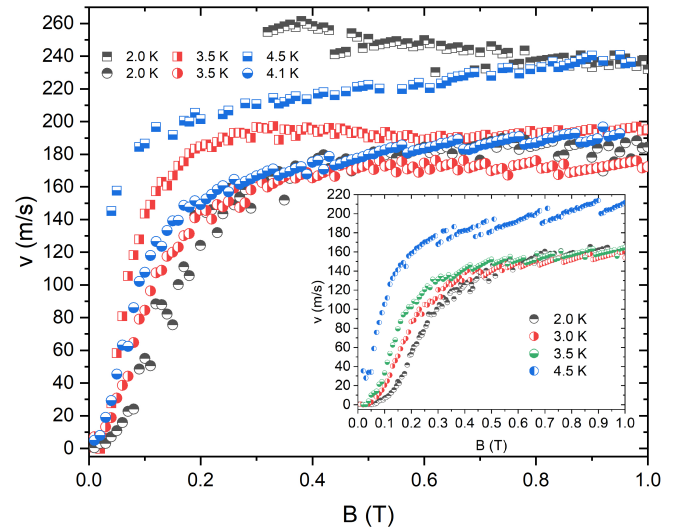


Fig. 5. Flux flow instability velocity as a function of out of the plane magnetic field for 2 devices of width  $4.8 \mu\text{m}$  (square) and  $2.2 \mu\text{m}$  (round symbol) measured at different temperatures. Inset shows the same measurements on a smaller device of  $1.8 \mu\text{m}$  width. Blue-coloured data were collected at near the critical temperatures of the devices.

The consistent values for the flow velocities across different oxidised devices suggest the change in film condition is homogeneous for all of them. This excludes the possibility that the flux is trapped by local defects that could be generated while fabricating individual devices. We propose that the dramatic decrease in the flux flow instability velocity, and hence the increase in quasiparticle relaxation times, is caused by the pinning of vortices. These pinning centres could exist at the domain wall of oxidised and unoxidized patches across the sample surface.

#### IV. ANALYSIS AND DISCUSSION

The properties of superconductors can often dramatically vary when the surface starts to oxidise [29] [30]. In our devices, we observe normal state resistivity and the critical temperature, defined as the temperature at zero resistance, to be comparable between the oxidised ( $240 \pm 10 \mu\Omega \text{ cm}$ ,  $4.21 \pm 0.01\text{K}$ ) and the original film ( $238 \pm 10 \mu\Omega \text{ cm}$ ,  $4.23 \pm 0.01\text{K}$  for the  $1.8 \mu\text{m}$  wide strip as an example). This indicates the modification of the film is very limited, although the light oxidation might lead to inhomogeneities of the film. However, there is an evident change in the film behaviour concerning critical current density as shown in the previous section. We explain our results by assuming that slight oxidation leads to part of the device gaining a different superconducting characteristic length than the rest. We propose a toy model in which the changes on the device surface act as pinning centres where the flux is likely to be trapped.



To support our claim, we perform simple time-dependent Ginzburg-Landau simulations with COMSOL Multiphysics to qualitatively illustrate our hypothesis. The time-dependent Ginzburg-Landau equations are [31]:

$$\frac{\partial \Psi}{\partial t} = -\left(\frac{i}{\kappa} \nabla + \mathbf{A}\right)^2 \Psi + \Psi - |\Psi|^2 \Psi \quad (1)$$

$$\sigma \frac{\partial \mathbf{A}}{\partial t} = \frac{1}{2i\kappa} (\Psi^* \nabla \Psi - \Psi \nabla \Psi^*) - |\Psi|^2 \mathbf{A} - \nabla \times (\nabla \times \mathbf{A} - \mathbf{B}) \quad (2)$$

With boundary conditions of:

$$\begin{aligned} \nabla \Psi \cdot \mathbf{n} &= 0 \\ \nabla \times \mathbf{A} &= \mathbf{B} \\ \mathbf{A} \cdot \mathbf{n} &= 0 \end{aligned} \quad (3)$$

Where  $\Psi$  is the order parameter,  $\mathbf{A}$  is the vector potential of the electromagnetic field,  $\sigma$  is the normalised normal state conductance,  $\kappa = \lambda/\xi$ ,  $\lambda$  is the penetration depth,  $\xi$  is the coherence length and  $\mathbf{B}$  is the applied magnetic field. A quantitative calculation of energy dissipation in an actual device is beyond the scope of this article. The detailed formulation of the numerical simulation has been published in [31]–[33].

It is important to note that we are only solving the partial differential equation for the superconducting wave function in the magnetic field at timescales where a steady-state is achieved. In these calculations, there is no superconducting current direction, and we are not varying the amount of current sustained in the system. The loss of energy from the system or the flow of the flux when the current is increased in the system cannot be obtained from such calculations. Instead, the simulation models how flux enters the superconductor and diffuses into the energetically most favourable arrangement close to the device's critical current. Full simulation details can be found in reference [31].

Figure 6 shows the vortex distribution in a steady-state configuration for two superconductors that contain an area (the inner rectangle) with a different superconducting characteristic length. The simulations are done for value  $\kappa = 100$  obtained from the reported values for a 60 nm NbRe film [14]. The dimensions in the simulation are normalised with respect to the London penetration depth. For the case where the coherence length is larger in the inner rectangle, shown in Figure 6(b), the vortices are attracted to the domain wall to sustain the lowest energy configuration. The same happens at the corners of the rectangle in Figure 6(a).

We expect that as the current sustained in the superconductor increases, the vortex will have difficulty flowing across the boundaries, whereas the vortices that are trapped along the domain wall will experience less pinning in the flow. The energy dissipation measured across the whole device is the sum of the dissipation of all vortex motion. This implies that the calculated flux flow instability velocity in the oxidised devices is the average velocity of the vortex motion in all different regions. The quasiparticle relaxation time will also vary locally and depend non-linearly on the local flow velocity. For a wide distribution, it is no longer reasonable to use

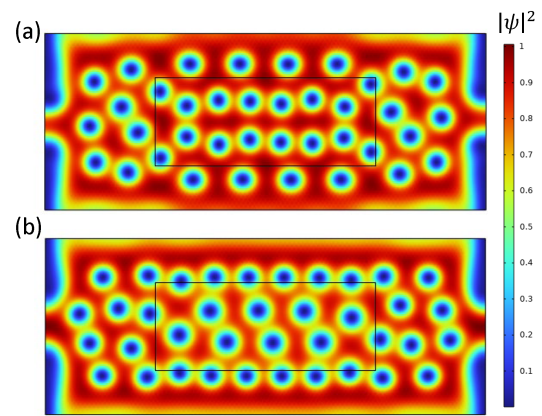


Fig. 6. False colour graph of superconducting order parameter under magnetic field simulated with time-dependent Ginzburg-Landau theory of a Type II superconductor with two regions that have different coherent lengths. The outer regions have a width of  $0.5\lambda$  and a length of  $0.2\lambda$ , and the inner regions have a width of  $0.25\lambda$  and a length of  $0.1\lambda$ . The outer region has  $\kappa = 100$  [14] [34]. In (a) the inner rectangle has  $\kappa = 110$  whereas in (b) the inner region has  $\kappa = 90$ .

the average velocity to calculate the average quasiparticle relaxation time.

We also want to point out that the tendency of vortices to be attracted to the boundary of two regions with different coherence lengths will increase the effect of pinning in the system. Accordingly, the overall velocity of flux motion is dramatically reduced. As the simulation applies to any type-II superconductor, we should expect a similar degradation effect in other polycrystalline systems that are prone to oxidation.

## V. CONCLUSION

We have investigated the effect of oxidation on the magnetic response of flux-flow behaviour in 8 nm thin superconducting NbRe films. A degradation of the film that we attribute to a slight oxidation dramatically decreases the flux flow instability velocity and therefore increases quasiparticle relaxation time. Our observations can be explained using a toy model where the domain wall between the oxidised area and clean area provides pinning forces for the vortices. Similar effects should be taken into account in other materials for fast and efficient photon-detecting techniques if these materials are sensitive to oxidation and/or surface modification.

## ACKNOWLEDGMENTS

This work was made possible by financial support from the Dutch Research Council (NWO) and Leiden University. The authors are grateful for the fruitful scientific discussion with Remko Fermin and Jan Aarts, and technical support from Marcel Hesselberth, Douwe Scholma, Federica Galli and Thomas Mechielsen.

## REFERENCES

- [1] M. Tinkham, *Introduction to Superconductivity*, 2nd ed. 31 East 2nd Street, Mineola, N.Y. 11501: Dover Publications, Inc., 2004.
- [2] S. Okuma, D. Shimamoto, and N. Kokubo, "Velocity-induced reorientation of a fast driven abrikosov lattice," *Phys. Rev. B*, vol. 85, p. 064508, Feb 2012. [Online]. Available: <https://link.aps.org/doi/10.1103/PhysRevB.85.064508>
- [3] A. Larkin and Y. Ovchinnikov, *Nonequilibrium Superconductivity*, 1st ed. Amsterdam: Elsevier, 1986.
- [4] Dobrovolskiy, O. V., Vodolazov, D. Yu, Porrati, F., Sachser, R., Bevez, V. M., Mikhailov, M. Yu, Chumak, A. V., Huth, M., "Ultra-fast vortex motion in a direct-write Nb-C superconductor," *Nat Commun*, vol. 11, no. 1, p. 3291, 2020.
- [5] I. Madan, J. Buh, V. V. Baranov, V. V. Kabanov, A. Mrzel, and D. Mihailovic, "Nonequilibrium optical control of dynamical states in superconducting nanowire circuits," *Science Advances*, vol. 4, no. 3, p. eaao0043, 2018. [Online]. Available: <https://www.science.org/doi/abs/10.1126/sciadv.aao0043>
- [6] G. Shaw, S. Blanco Alvarez, J. Brisbois, L. Burger, L. B. L. G. Pinheiro, R. B. G. Kramer, M. Motta, K. Fleury-Frenette, W. A. Ortiz, B. Vanderheyden, and A. V. Silhanek, "Magnetic recording of superconducting states," *Metals*, vol. 9, no. 10, 2019. [Online]. Available: <https://www.mdpi.com/2075-4701/9/10/1022>
- [7] D. Henrich, P. Reichensperger, M. Hofherr, J. M. Meckbach, K. Il'in, M. Siegel, A. Semenov, A. Zotova, and D. Y. Vodolazov, "Geometry-induced reduction of the critical current in superconducting nanowires," *Phys. Rev. B*, vol. 86, p. 144504, Oct 2012. [Online]. Available: <https://link.aps.org/doi/10.1103/PhysRevB.86.144504>
- [8] Y. N. O. A. I. Larkin, "Nonlinear conductivity of superconductors in the mixed state," *Sov. Phys.-JETP*, vol. 41, no. 5, pp. 1915–1927, May 1975.
- [9] G. Grimaldi, A. Leo, P. Sabatino, G. Carapella, A. Nigro, S. Pace, V. V. Moshchalkov, and A. V. Silhanek, "Speed limit to the abrikosov lattice in mesoscopic superconductors," *Phys. Rev. B*, vol. 92, p. 024513, Jul 2015. [Online]. Available: <https://link.aps.org/doi/10.1103/PhysRevB.92.024513>
- [10] A. V. Silhanek, A. Leo, G. Grimaldi, G. R. Berdiyrov, M. V. Milošević, A. Nigro, S. Pace, N. Verellen, W. Gillijns, V. Metlushko, B. Ilić, X. Zhu, and V. V. Moshchalkov, "Influence of artificial pinning on vortex lattice instability in superconducting films," *New Journal of Physics*, vol. 14, no. 5, p. 053006, may 2012. [Online]. Available: <https://dx.doi.org/10.1088/1367-2630/14/5/053006>
- [11] G. Grimaldi, A. Leo, A. Nigro, S. Pace, A. A. Angrisani, and C. Attanasio, "Flux flow velocity instability in wide superconducting films," *Journal of Physics: Conference Series*, vol. 97, no. 1, p. 012111, feb 2008. [Online]. Available: <https://dx.doi.org/10.1088/1742-6596/97/1/012111>
- [12] N. Haberkorn, "Thickness dependence of the flux-flow velocity and the vortex instability in nanocrystalline -Mo2N thin films," *Thin Solid Films*, vol. 759, p. 139475, 2022. [Online]. Available: <https://www.sciencedirect.com/science/article/pii/S004060902200387X>
- [13] G. Grimaldi, A. Leo, A. Nigro, A. V. Silhanek, N. Verellen, V. V. Moshchalkov, M. V. Milošević, A. Casaburi, R. Cristiano, and S. Pace, "Controlling flux flow dissipation by changing flux pinning in superconducting films," *Applied Physics Letters*, vol. 100, no. 20, p. 202601, 05 2012.
- [14] C. Cirillo, G. Carapella, M. Salvato, R. Arpaia, M. Caputo, and C. Attanasio, "Superconducting properties of noncentrosymmetric NbRe thin films probed by transport and tunnelling experiments," *Phys. Rev. B*, vol. 94, p. 104512, Sep 2016. [Online]. Available: <https://link.aps.org/doi/10.1103/PhysRevB.94.104512>
- [15] M. Caputo, C. Cirillo, and C. Attanasio, "NbRe as candidate material for fast single photon detection," *Applied Physics Letters*, vol. 111, no. 19, p. 192601, 11 2017. [Online]. Available: <https://doi.org/10.1063/1.4997675>
- [16] C. Cirillo, J. Chang, M. Caputo, J. W. N. Los, S. Dorenbos, I. Esmail Zadeh, and C. Attanasio, "Superconducting nanowire single photon detectors based on disordered NbRe films," *Applied Physics Letters*, vol. 117, no. 17, p. 172602, 10 2020. [Online]. Available: <https://doi.org/10.1063/5.0021487>
- [17] M. Ejmaes, C. Cirillo, D. Salvoni, F. Chianese, C. Brusino, P. Ercolano, A. Cassinese, C. Attanasio, G. P. Pepe, and L. Parlato, "Single photon detection in NbRe superconducting microstrips," *Applied Physics Letters*, vol. 121, no. 26, p. 262601, 12 2022. [Online]. Available: <https://doi.org/10.1063/5.0131336>
- [18] P. Ercolano, C. Cirillo, M. Ejmaes, F. Chianese, D. Salvoni, C. Brusino, R. Satariano, A. Cassinese, C. Attanasio, G. P. Pepe, and L. Parlato, "Investigation of dark count rate in NbRe microstrips for single photon detection," *Superconductor Science and Technology*, vol. 36, no. 10, p. 105011, sep 2023.
- [19] C. Zhang, W. Zhang, J. Huang, L. You, H. Li, C. Lv, T. Sugihara, M. Watanabe, H. Zhou, Z. Wang, and X. Xie, "NbN superconducting nanowire single-photon detector with an active area of 300 m-in-diameter," *AIP Advances*, vol. 9, no. 7, p. 075214, 07 2019. [Online]. Available: <https://doi.org/10.1063/1.5095842>
- [20] X. Yang, L. You, L. Zhang, C. Lv, H. Li, X. Liu, H. Zhou, and Z. Wang, "Comparison of superconducting nanowire single-photon detectors made of NbTiN and NbN thin films," *IEEE Transactions on Applied Superconductivity*, vol. 28, no. 1, pp. 1–6, 2018.
- [21] S. Miki, T. Yamashita, H. Terai, and Z. Wang, "High performance fiber-coupled NbTiN superconducting nanowire single photon detectors with gifford-mcmahon cryocooler," *Opt. Express*, vol. 21, no. 8, pp. 10208–10214, Apr 2013. [Online]. Available: <https://opg.optica.org/oe/abstract.cfm?URI=oe-21-8-10208>
- [22] V. B. Verma, B. Korzh, F. Bussières, R. D. Horansky, S. D. Dyer, A. E. Lita, I. Vayshenker, F. Marsili, M. D. Shaw, H. Zbinden, R. P. Mirin, and S. W. Nam, "High-efficiency superconducting nanowire single-photon detectors fabricated from MoSi thin-films," *Opt. Express*, vol. 23, no. 26, pp. 33792–33801, Dec 2015. [Online]. Available: <https://opg.optica.org/oe/abstract.cfm?URI=oe-23-26-33792>
- [23] B. Korzh, Q.-Y. Zhao, S. Frasca, D. Zhu, E. Ramirez, E. Bersin, M. Colangelo, A. E. Dane, A. D. Beyer, J. Allmaras, E. E. Wollman, K. K. Berggren, and M. D. Shaw, "WSi superconducting nanowire single photon detector with a temporal resolution below 5 ps," in *Conference on Lasers and Electro-Optics*. Optica Publishing Group, 2018, p. FW3F.3. [Online]. Available: [https://opg.optica.org/abstract.cfm?URI=CLEO\\_QELS-2018-FW3F.3](https://opg.optica.org/abstract.cfm?URI=CLEO_QELS-2018-FW3F.3)
- [24] C. Cirillo, M. Caputo, G. Divitini, J. Robinson, and C. Attanasio, "Polycrystalline NbRe superconducting films deposited by direct current magnetron sputtering," *Thin Solid Films*, vol. 758, p. 139450, 2022.
- [25] W. Klein, R. P. Huebener, S. Gauss, and J. Parisi, "Nonlinearity in the flux-flow behavior of thin-film superconductors," *Journal of Low Temperature Physics*, vol. 61, no. 5, pp. 413–432, 1985.
- [26] B. Budinská, B. Aichner, D. Y. Vodolazov, M. Y. Mikhailov, F. Porrati, M. Huth, A. Chumak, W. Lang, and O. Dobrovolskiy, "Rising speed limits for fluxons via edge-quality improvement in wide mosi thin films," *Phys. Rev. Appl.*, vol. 17, p. 034072, Mar 2022. [Online]. Available: <https://link.aps.org/doi/10.1103/PhysRevApplied.17.034072>
- [27] C. Cirillo, V. Pagliarulo, H. Myoren, C. Bonavolontà, L. Parlato, G. P. Pepe, and C. Attanasio, "Quasiparticle energy relaxation times in NbN/CuNi nanostrips from critical velocity measurements," *Phys. Rev. B*, vol. 84, p. 054536, Aug 2011. [Online]. Available: <https://link.aps.org/doi/10.1103/PhysRevB.84.054536>
- [28] G. Grimaldi, A. Leo, A. Nigro, S. Pace, A. A. Angrisani, and C. Attanasio, "Flux flow velocity instability in wide superconducting films," *Journal of Physics: Conference Series*, vol. 97, no. 1, p. 012111, feb 2008. [Online]. Available: <https://dx.doi.org/10.1088/1742-6596/97/1/012111>
- [29] L. Zhang, L. You, L. Ying, W. Peng, and Z. Wang, "Characterization of surface oxidation layers on ultrathin NbTiN films," *Physica C: Superconductivity and its Applications*, vol. 545, pp. 1–4, 2018. [Online]. Available: <https://www.sciencedirect.com/science/article/pii/S0921453417300588>
- [30] M. D. Henry, S. Wolfley, T. Young, T. Monson, C. J. Pearce, R. Lewis, B. Clark, L. Brunke, and N. Missert, "Degradation of superconducting Nb/NbN films by atmospheric oxidation," *IEEE Transactions on Applied Superconductivity*, vol. 27, no. 4, pp. 1–5, 2017.
- [31] P. N. F. M. S. Alstrøm, Tommy Sonne, Sørensen, Mads Peter, "Magnetic Flux Lines in Complex Geometry Type-II Superconductors Studied by the Time Dependent Ginzburg-Landau Equation," *Acta Applicandae Mathematicae*, vol. 115, no. 1, pp. 63–74, 7 2011. [Online]. Available: <https://doi.org/10.1007/s10440-010-9580-8>
- [32] D. Lu, "Vortex dynamics in type ii superconductors," 2017.
- [33] Q. Du, "Finite element methods for the time-dependent ginzburg-landau model of superconductivity," *Computers Mathematics with Applications*, vol. 27, no. 12, pp. 119–133, 1994. [Online]. Available: <https://www.sciencedirect.com/science/article/pii/0898122194900914>
- [34] Z. M. Kakhaki, A. Leo, F. Chianese, L. Parlato, G. P. Pepe, A. Nigro, C. Cirillo, and C. Attanasio, "Upper critical magnetic field in nbre and nbren micrometric strips," *Beilstein Journal of Nanotechnology*, vol. 14, pp. 45–51, 2023. [Online]. Available: <https://doi.org/10.3762/bjnano.14.5>